Parallel computation on the fluid flow and heat transfer in the confined jet flow in the presence of magnetic field

H. G. Lee[a], M. Y. Ha[b]* and H. S. Yoon[c]

[a] Air conditioning Division, LG Electronics Co., 76 Sungsan, Changwon, Korea
[b*] School of Mechanical Engineering, Pusan National University San 30, Chang Jeon Dong, Kum Jeong Gu, Pusan 609-735, Korea
[c] Advanced Ship Engineering Rsearch Center, Pusan National University San 30, Chang Jeon Dong, Kum Jeong Gu, Pusan 609-735, Korea

Key Words: MPI (Message Passing Interface), Jet flow, Magnetic Field

ABSTRACT

The present study numerically investigates two-dimensional fluid flow and heat transfer in the confined jet flow in the presence of applied magnetic field. For the purpose of controlling vortex shedding and heat transfer, numerical simulations to calculate the fluid flow and heat transfer in the confined jet are performed for different Reynolds numbers in the absence and presence of magnetic fields and for different Prandtl numbers of 0.02 (liquid metal), 0.7 (air) and 7 (water) in the range of $0 \le N \le 0.05$, where N is the Stuart number (interaction parameter) which is the ratio of electromagnetic force to inertia force. The present study reports the detailed information of flow and thermal quantities in the channel at different Stuart numbers. As the intensity of applied magnetic fields increases, the vortex shedding formed in the channel becomes weaker and the oscillating amplitude of impinging jet decreases. The flow and thermal fields become the steady state if the Stuart number is greater than the critical value. Thus the pressure coefficients and Nusselt number at the stagnation point representing the fluid flow and heat transfer characteristics also vary as a function of Stuart number.

Figure 1 shows the computational domain and coordinate system for a two-dimensional confined impinging jet considered in the present study. We solve the unsteady two-dimensional dimensionless continuity, Navier-Stokes and energy equations defined as

$$\nabla \cdot \vec{u} = 0, \quad \text{- (1)} \qquad \frac{\partial \vec{u}}{\partial t} + \vec{u} \cdot \nabla \vec{u} = -\nabla p + \frac{1}{Re} \nabla^2 \vec{u} + \vec{f} \quad \text{- (2)} \qquad \frac{\partial T}{\partial t} + \vec{u} \cdot \nabla T = \frac{1}{Re \cdot Pr} \nabla^2 T \quad \text{-(3)}$$

The above non-dimensionalization results in two dimensionless parameters: $Re = V_{jet} D / \nu$ and $Pr = \nu / \alpha$ where ν and α are the kinematic viscosity and thermal diffusivity. In the simulations to be reported here the Prandtl number, Pr, has been taken to be 0.02, 0.7 and 7 corresponding to liquid metal, air and water, respectively.

We assume that the magnetic field is parallel to the z-direction with constant values and as a result the Lorentz force $\vec{f}$ used in equation (2) and acting on the fluid is defined as follows [1~3].

$$\vec{f} = N(\vec{J} \times e_z) \quad \text{- (5)}; \quad \nabla \cdot \vec{J} = 0 \quad \text{- (6)}; \quad \vec{J} = -\nabla \phi + \vec{u} \times e_z \quad \text{- (7)}; \quad \nabla^2 \phi = \nabla \cdot \left(\vec{u} \times e_z \right) \quad \text{- (8)}$$

Using equation (6) and (7), we can derive a Possion equation (8). The Poisson equation is solved to get the electric potential ϕ. The Lorentz force in the momentum equation (2) induced by the magnetic field is obtained by using equation (5). Here we can define additional dimensionless parameter called as Stuart number or interaction parameter, which is the ratio of electromagnetic force to inertia force, as follows:

$$N = \sigma B_0^2 D / (\rho V_{jet}) \tag{9}$$

where σ and B_0 represent electric conductivity and external magnetic field.

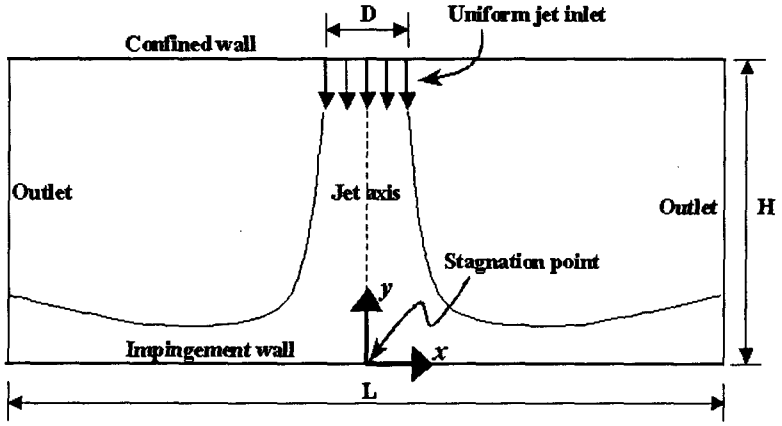

Figure 1. Computational domain and coordinate system for a two-dimensional confined impinging jet.

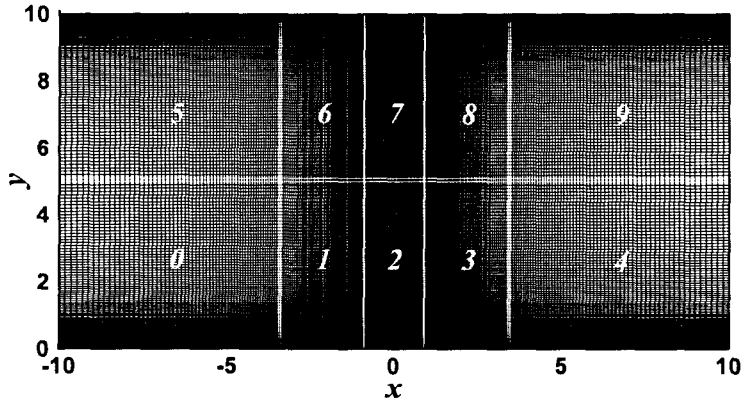

Figure 2. Grid distribution and the number of domain used

Figure 2 shows the grid distribution and the number of domain used in the present study. The number of grid points used in the present calculation is 301×201 ($x \times y$) and the number of domain used is 10. Grid independence of the solution has been confirmed with additional simulations on much less and finer grids. The condition of $CFL < 0.3$ is chosen to determine the non-dimensional time step used in the present calculations. The computations are advanced in time until it is observed that the pressure and heat transfer coefficients have reached a statistically stationary state. The developed computer code is parallelized based on the MPI (Message Passing Interface) to increase the computational speed [4]. The number of processors used is 5 in the x-direction and 2 in the y-direction, respectively, as shown in Fig. 2. The same number of grid points is allocated to each processor.

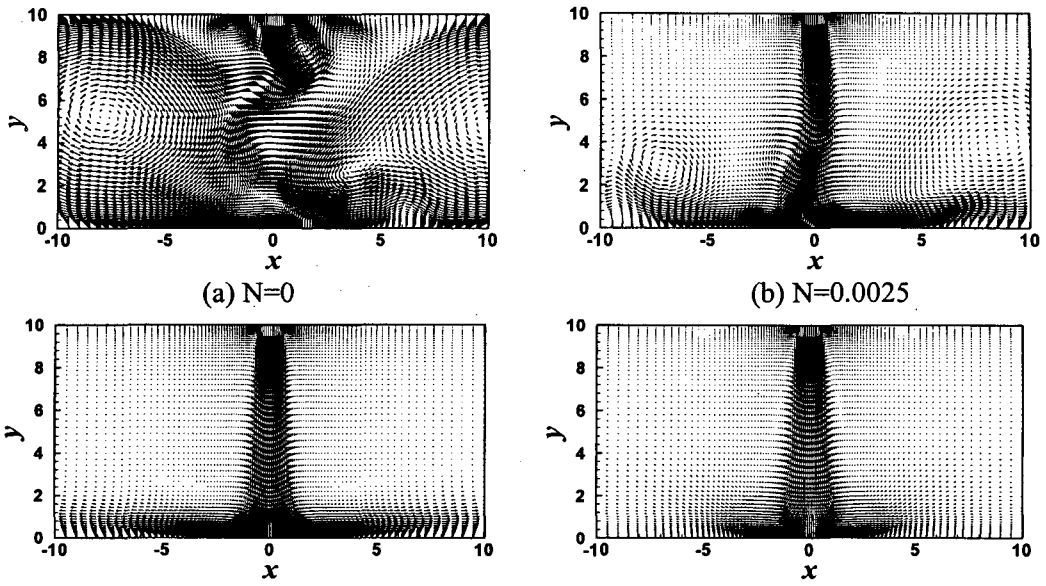

Figure 3. Instantaneous velocity vectors at $Re = 250$ and $H/D = 10$ for different N values.

Figure 3 shows the instantaneous velocity vectors at $Re = 250$ and $H/D = 10$ for different N values in the presence of magnetic fields. Fig. 3(a) shows the instantaneous velocity vector for $N = 0$ corresponding to the case without the applied magnetic field to compare its results with those for the case in the presence of magnetic fields. If the constant magnetic fields are applied to the confined impinging jet in the z-direction, the forces induced by the magnetic fields act on the jet flow in the opposite direction and damp the movement of jet flow. When $N = 0.0025$ corresponding to the weak magnetic field, the instantaneous flow field is still time-dependent and shows a non-symmetric pattern similar to the case of $N = 0$. If N is increased further to 0.005, the unsteadiness of flow is very weak. As a result the jet flow approaches to the steady state and shows almost the symmetric pattern. When the magnetic field is strong as $N \geq 0.01$, the jet flow becomes steady and symmetric. The pattern of jet flow for $N \geq 0.01$ is very similar to that of steady jet flow obtained at the lower Reynolds number. When $N = 0.03$, the applied magnetic field is so strong that the jet flow can not arrive at the stagnation point at the lower wall at the Reynolds number of 250 due to the strong Lorentz force

Figures 4 show the instantaneous wall pressure coefficients and Nusselt number ($C_{p,stag}$ and Nu_{stag}) for different Prandtl numbers of 0.02, 0.7 and 7 at the stagnation point, respectively, for different values of N as a function of dimensionless time at $H/D = 10$ and $Re = 250$. The time history of $C_{p,stag}$ and Nu_{stag} during the dimensionless time of $1400 \leq t \leq 1500$ corresponds to the case without applied magnetic fields ($N = 0$). The flow and temperature fields at $t = 1500$ for the case of $N = 0$ are used as initial conditions to calculate the fluid flow and temperature fields in the presence of applied magnetic fields. The value itself of Nu_{stag} for both cases with and without applied magnetic fields increases with increasing Prandtl number because the thermal boundary layer thickness and thermal gradient on the lower wall increase. However, when the time history of Nu_{stag} changes its shape from the unsteady to the steady pattern as N increases in the presence of magnetic fields, the general trend in the change of Nu_{stag} is generally similar for different Prandtl numbers. If we apply the magnetic field of $N = 0.0025$, the flow is still time-dependent, but the unsteadiness and the oscillating

amplitude of $C_{p,stag}$ and Nu_{stag} decrease very quickly due to the damping effect of applied magnetic fields, compared to the case of $N = 0$ in the absence of applied magnetic field. When the applied magnetic fields increase above $N \geq 0.005$, the flow approaches the steady state, and $C_{p,stag}$ and Nu_{stag} for all three cases of Pr=0.02, 0.7 and 7 reach the constant value.

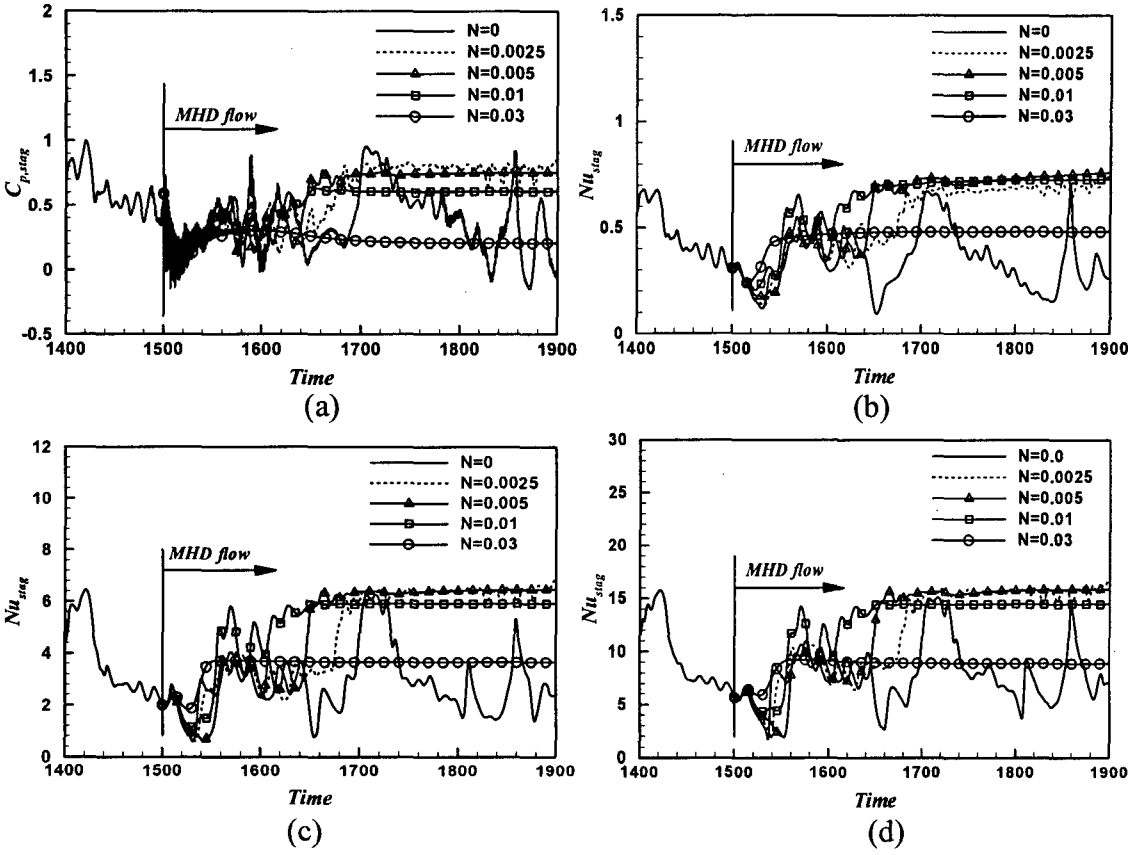

Figure 4. Instantaneous wall pressure coefficient (a) ($C_{p,stag}$) and Nusselt number at the stagnation point (Nu_{stag}) as a function of time for different N values at $H/D = 10$ and $Re = 250$. (b) $Pr = 0.02$, (c) $Pr = 0.7$, (d) $Pr = 7$.

REFERENCES

[1] M.Y. Ha, H.G. Lee, S.H. Seong, (2003). 밙umerical simulation of three-dimensional flow, heat transfer, and solidification of steel in continuous casting mold with electromagnetic brake? *J. Material Processing Tech.* Vol. **133**. pp.322-339.

[2] B. M? k, C. G? ther, U. M? ler, L. B? ler, (2000). 빷hree-dimensional MHD flows in rectangular ducts with internal obstacles? *J. Fluid Mech.* Vol. **418.** 265-295.

[3] H.S. Yoon, H.H. Chun, M.Y. Ha, H.G.. Lee, (2004). 밇 numerical study on the fluid flow and heat transfer around a circular cylinder in an aligned magnetic fields , *Int. J. Heat Mass Transfer* Vol. **47** 4075-4087.

[4] P.S. Pacheco, (1997). 밙arallel programming with MPI? *Morgan kaufmann Publishers Inc.*